Raman study of twin-free ortho-II $YBa_2Cu_3O_{6.5}$ single crystals

M. N. Iliev and V. G. Hadjiev
Texas Center for Superconductivity, University of Houston, Texas 77204-5002, USA

S. Jandl and D. Le Boeuf
Regroupement Québecois sur les Matériaux de Pointe, Département de Physique, Université de Sherbrooke, Sherbrooke, Canada J1K 2R1

V. N. Popov
Faculty of Physics, University of Sofia, 1164 Sofia, Bulgaria

D. Bonn, R. Liang, and W. N. Hardy
Department of Physics and Astronomy, University of British Columbia, Vancouver, British Columbia, Canada V6T 1Z1

(Received 20 February 2008; revised manuscript received 17 April 2008; published 19 May 2008)

The polarized Raman scattering spectra from freshly cleaved *ab*, *ac*, and *bc* surfaces of high quality twin-free $YBa_2Cu_3O_{6.5}$ (ortho-II) single crystals (T_c=57.5 K and ΔT=0.6 K) were studied between 80 and 300 K. All 11 A_g Raman modes expected for the ortho-II structure as well as some modes of B_{2g} and B_{3g} symmetries were identified in close comparison to predictions of lattice dynamical calculations. The electronic scattering from the *ab* planes is strongly anisotropic and decreases between 200 and 100 K within the temperature range of a previously reported pseudogap opening. The coupling of phonons to Raman active electronic excitations manifested by asymmetric (Fano) profiles of several modes also decreases within the same range. Among the findings that distinguish the Raman scattering of the ortho-II phase from that of the ortho-I phase is the unusual relationship ($\alpha_{xx} \approx -\alpha_{yy}$) between the elements of the Raman tensor of the apex oxygen A_g mode.

DOI: 10.1103/PhysRevB.77.174302 PACS number(s): 78.30.−j, 74.25.Kc, 74.72.Bk

I. INTRODUCTION

The properties of underdoped $YBa_2Cu_3O_x$ ($6<x<7$) have been intensively studied within the efforts to unravel the mechanism of high temperature superconductivity. The ortho-II phase, which corresponds to the oxygen content $x=6.5$ and is characterized by alternating full and empty chains, has attracted particular attention as it is both underdoped and free of disorder. Although the existence of this phase has been experimentally documented in a considerable number of reports, it has also been established that as a rule the ortho-II domains coexist with domains of different oxygen orderings and/or strong disorder, even in the case where $x \simeq 6.5$. An improved procedure developed by Liang *et al.*[1] has made possible the preparation of twin-free, highly ordered ortho-II single crystals. Such crystals have recently been used in several studies of specific properties of the ortho-II phase by means of neutron scattering,[2,3] x-ray diffraction,[4] time-resolved spectroscopy,[5,6] infrared spectroscopy,[7] nuclear magnetic resonance,[8] microwave spectroscopy,[9] and resistance measurements in high magnetic fields.[10]

There have been several attempts to identify the Raman modes of the ortho-II phase by measuring the spectra of oxygen deficient $YBa_2Cu_3O_x$ ($x \approx 6.5$) single crystals.[11–13] Compared to the well known Raman spectra of the ortho-I ($x=7$) and the T ($x=6$) phases, in the case of the ortho-II phase, one expects a shift in the corresponding Raman modes and the activation of additional modes due to the doubling of the unit cell. A significant number of additional modes have been observed, but their identification has met definite difficulties due to ambiguities in the local structure of $YBa_2Cu_3O_x$, even in the case where $x=6.5$. Indeed, in the idealized ortho-I, ortho-II, and T structures, the Cu1 and O1 atoms in the basal Cu-O planes are at centrosymmetrical sites and their vibrations are not Raman active. The oxygen arrangement in the basal planes of a real $YBa_2Cu_3O_x$ material, however, is characterized by chain fragments instead of infinite chains, and part of the oxygen atoms are outside the chains in otherwise vacant O5 sites. This creates a number of local noncentrosymmetrical surroundings for the Cu and O atoms, in particular those at the end of the chain fragments, and activates their vibrations in the Raman spectrum.[13,14] Some of these defects can also be produced by local laser annealing[15,16] or photoactivation.[17] Another issue, as a rule neglected but of particular importance in the case of the ortho-II phase, is the possible lack of correspondence between the oxygen content and the arrangement in the volume of the crystal and its surface layer(s), where the Raman scattering occurs. The cause for such discrepancy is the in- and out-diffusion of oxygen, which strongly depends on the type of surface (*ab*, *bc*, or *ac*), starting oxygen content, ambient oxygen pressure, temperature, and exposure time.[18,19]

In this paper, we present the results of a temperature-dependent Raman study of freshly cleaved *ab*, *ac*, and *bc* surfaces of a twin-free $YBa_2Cu_3O_{6.5}$ (YBCO6.5) single crystal with a high degree of ortho-II type ordering. This allowed us with great certainty to identify the proper Raman modes of the ortho-II phase and assign them to definite atomic motions via a close comparison to predictions of lattice dynami-

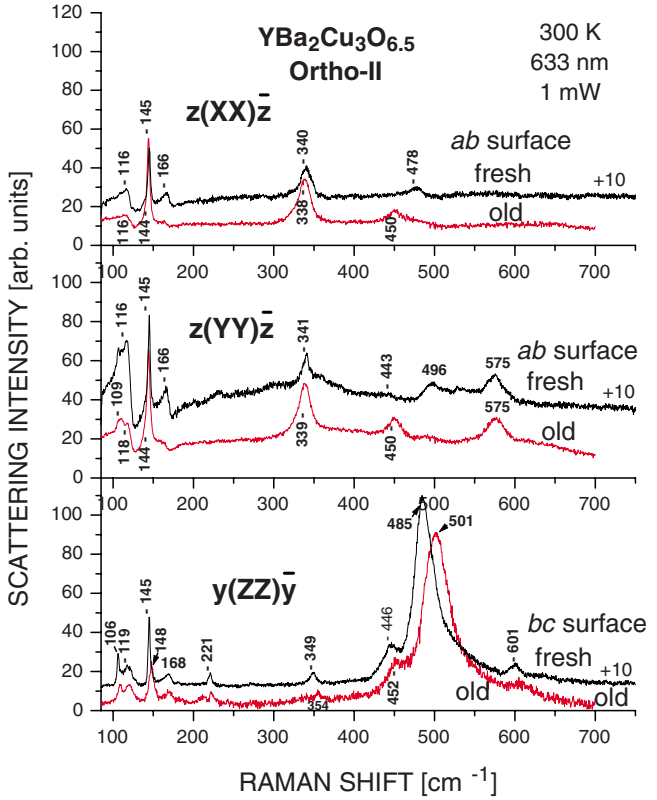

FIG. 1. (Color online) Raman spectra of $YBa_2Cu_3O_{6.5}$ (ortho-II) obtained from freshly cleaved and aged *ab* and *bc* surfaces.

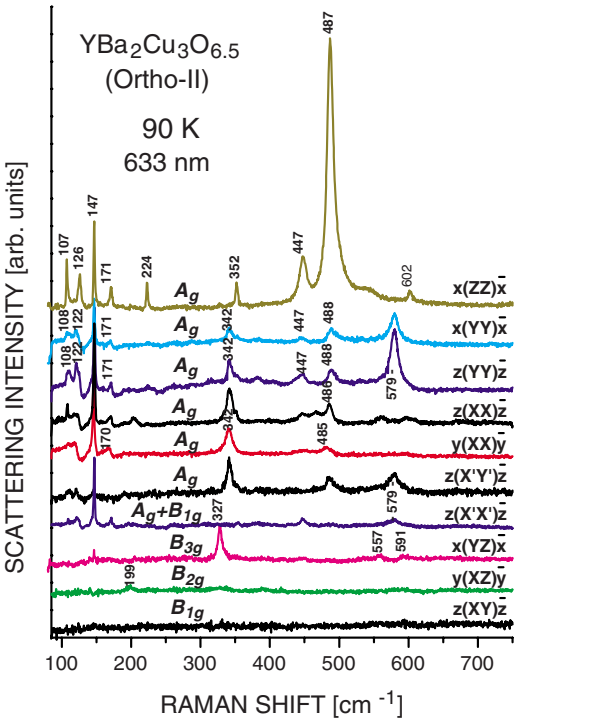

FIG. 2. (Color online) Raman spectra of $YBa_2Cu_3O_{6.5}$ (ortho-II) obtained at 90 K from freshly cleaved *ab*, *ac*, and *bc* surfaces. The spectra are vertically shifted for clarity.

cal calculations, as well as to measure the symmetry and strength of the electronic scattering.

II. SAMPLES AND EXPERIMENT

We used a high quality mechanically detwinned ortho-II YBCO6.5 single crystal with T_c=57.5 K and ΔT=0.6 K, which had been grown 1 yr earlier by a flux method in a $BaZrO_3$ crucible.[1,10] Immediately before mounting the sample on the cold finger of a Microstat®He (Oxford Instruments) optical cryostat, a small area of the as grown surface (*ab*, *ac*, or *bc*) to be used for Raman measurements was cleaved out to ensure that the scattering volume has an ortho-II oxygen arrangement. The Raman spectra were measured under a microscope (×50 magnification) by using a triple T64000 (Horiba Jobin Yvon) spectrometer. In most of the experiments, we used 633 nm excitation with a less than 1 mW incident laser power focused at a spot of 2–3 μm diameter. Comparative measurements with 515, 488, and 458 nm excitations were also done. All of the spectra were corrected for the Bose factor. All precautions were taken to account for the polarization properties of the setup and avoid spurious signals. For the description of the scattering configurations, we use the Porto notation $a(BC)d$, where the first and fourth letters denote, respectively, the directions of incident and scattered light in a Cartesian *xyz* system with the axes along the crystallographic directions. The polarization of the incident and scattered light is given by the second and third letters, respectively.

III. RESULTS AND DISCUSSION

A. Raman phonons in the ortho-II phase

Compared in Fig. 1 are the Raman spectra obtained with 633 nm excitation at room temperature from the freshly cleaved and aged as grown areas on the *ab* and *bc* surfaces of the same ortho-II crystal. The spectral shapes and Raman line frequencies from the 1-yr-aged surfaces are consistent with those from earlier reports on the *XX*/*YY* and *ZZ* spectra of twinned YBCO6.5[12] and $YBCO_x$ ($x \approx 6.5$) samples.[20–22] The corresponding spectra from the freshly cleaved and aged surfaces, however, exhibit definite differences in the positions and appearance of some of the peaks.

Figure 2 shows the Raman spectra from the freshly cleaved surfaces at 90 K in all available exact scattering configurations. From symmetry considerations, for the ortho-II structure one expects an increased number of Raman active modes, $11A_g+4B_{1g}+11B_{2g}+8B_{3g}$, compared to the $5A_g+5B_{2g}+5B_{3g}$ modes of the ortho-I structure. The atomic displacements of the 11 A_g modes, as predicted by lattice dynamical calculations (LDCs),[13] are shown in Fig. 3. For most modes, the experimentally observed frequencies (at 90 K) are in good agreement with those predicted by LDCs, which are shown in parentheses. In addition to the five A_g modes at 126, 147, 342, 447, and 487 cm^{-1}, which correspond to displacements along the *c* axis of Ba, Cu2, O2-O3, O2+O3, and O4 in the ortho-I structure, there are six more A_g modes in the extended ortho-II cell. Four of them can be positively identified at 107 cm^{-1} [$Cu2(z)-Cu2'(-z)$ out of phase], 171 cm^{-1} [$Y(x)$], 352 cm^{-1} [$O4(z)-O4'(-z)$ out of phase], and 579 cm^{-1} [$O2(x)$]. The mixed Ba/Cu mode,

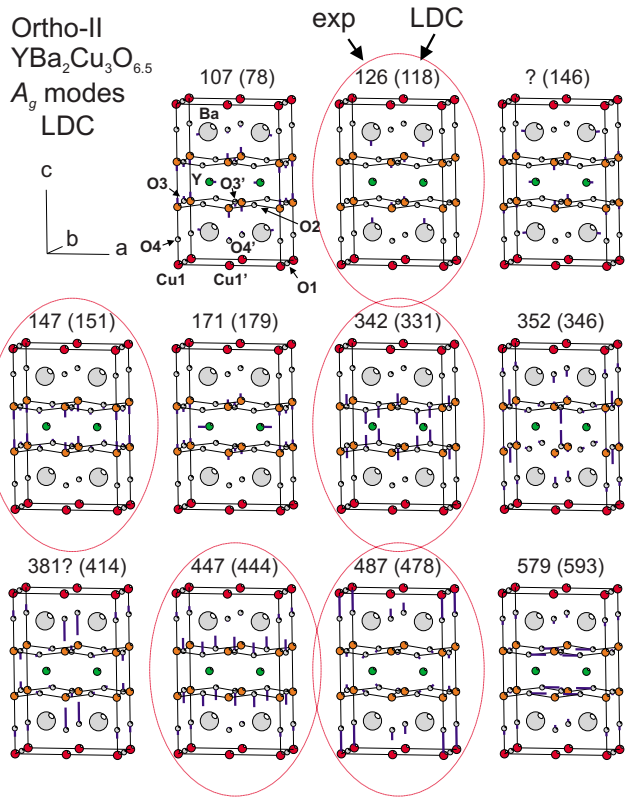

FIG. 3. (Color online) Main atomic displacements of the A_g modes of $YBa_2Cu_3O_{6.5}$ (ortho-II) as obtained by LDCs. The LDC predicted frequencies (in parentheses) are compared to the experimentally obtained values.

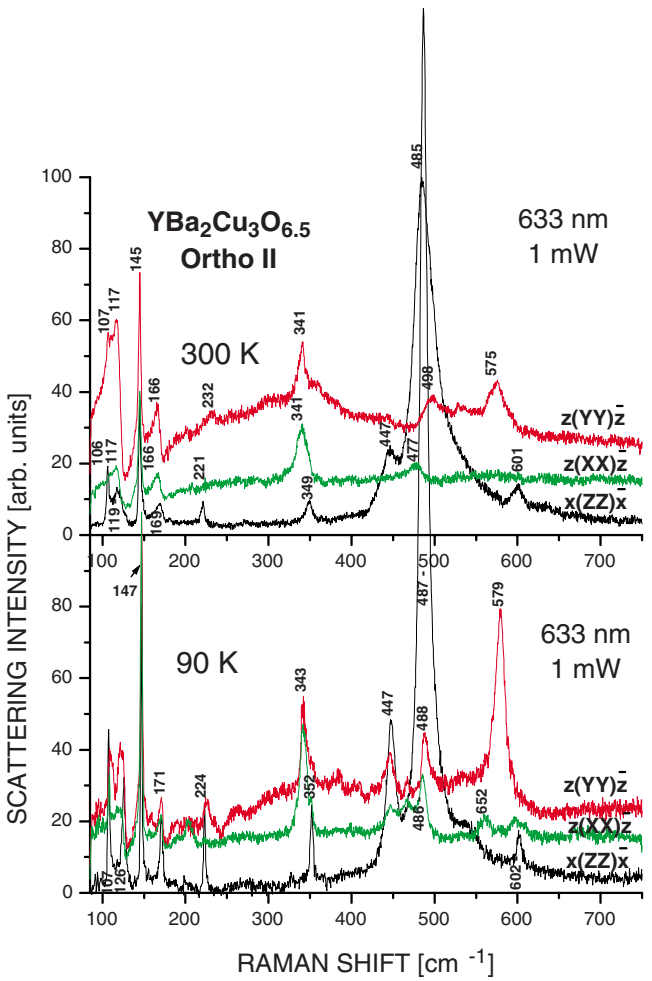

FIG. 4. (Color online) $z(XX)\bar{z}$, $z(YY)\bar{z}$, and $y(ZZ)\bar{y}$ spectra of ortho-II at 300 and 90 K. Note the asymmetric Fano shape of the Ba (117 cm^{-1}), Y (166 cm^{-1}), and apex oxygen (477 and 498 cm^{-1}) modes in the XX and YY spectra at 300 K.

which is predicted at 146 cm^{-1}, may be very weak and not observable. The weak Raman line at 381 cm^{-1} can be tentatively assigned to the mode involving mainly O4′ displacements along c, with a predicted frequency of 414 cm^{-1}. In the ZZ spectra, one observes additional lines of A_g character at 224 and 601 cm^{-1}. These positions are close to those of defect modes related to displacements of Cu1 and O1 at the end of broken chains,[13,15,21] which could preexist or be created by photoactivation in our ortho-II sample.

In the $XZ(B_{2g})$ and $YZ(B_{3g})$ spectra, one observes relatively strong Raman peaks at 199 and 327 cm^{-1}, respectively. The closest B_{2g} (200 and 213 cm^{-1}) and B_{3g} (300 cm^{-1}) frequencies predicted by LDCs correspond to modes involving mainly displacements of O4 and O4′ along the a and b directions, respectively.

A more careful look at the appearance of the apex oxygen mode near 487 cm^{-1} in the $X'X'$ and $X'Y'$ spectra of Fig. 2 reveals a significantly different behavior compared to that of the corresponding spectra of the ortho-I phase. Indeed, with these scattering configurations, the intensity of an A_g Raman line is proportional to $(\alpha_{xx}+\alpha_{yy})^2$ and $(\alpha_{xx}-\alpha_{yy})^2$, respectively, where α_{xx} and α_{yy} are diagonal elements of the corresponding Raman tensors. A negligible intensity in the $X'X'$ spectra may be expected if $\alpha_{xx}\approx-\alpha_{yy}$, which in the ortho-I phase is satisfied only for the out-of-phase O2-O3 mode at ≈336 cm^{-1} but not for the apex oxygen mode near 500 cm^{-1} (seen in the $X'X'$ spectrum but not in the $X'Y'$ spectrum). Here, for the ortho-II phase, the apex oxygen mode has an appearance similar to that of the out-of-phase mode: it is practically not seen in the $X'X'$ spectrum but is well pronounced in the $X'X'$ spectrum with an intensity comparable to that in the XX and the YY spectra. This allows us to conclude that for the apex oxygen mode of the ortho-II phase, the relation $\alpha_{xx}\approx-\alpha_{yy}$ is satisfied.

B. Electronic scattering and electron-phonon interaction

In addition to discrete phonon lines, the Raman spectra of the ortho-II phase contain a structureless background with an intensity stronger with YY than with XX and a negligible intensity with ZZ polarization (Fig. 4). Such background scattering, which is observed in the normal and superconducting states of high T_c superconductors, has been attributed to electronic scattering and has been intensively studied both experimentally and theoretically.[23–26] It has been shown that for optimally doped YBCO, the electronic scattering is practically independent of temperature for $T>T_c$. With the opening of a superconducting gap Δ at $T<T_c$, there is a redistribution of electronic scattering intensities from lower to higher energies and a maximum associated with pair break-

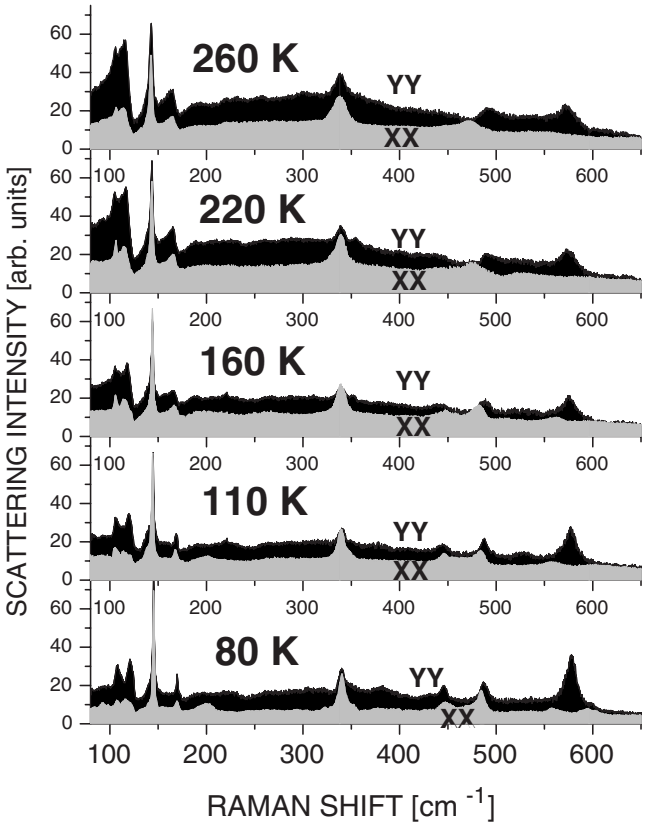

FIG. 5. Variation in the electronic background in the $z(XX)\bar{z}$ and $z(YY)\bar{z}$ spectra of ortho-II between 260 and 80 K.

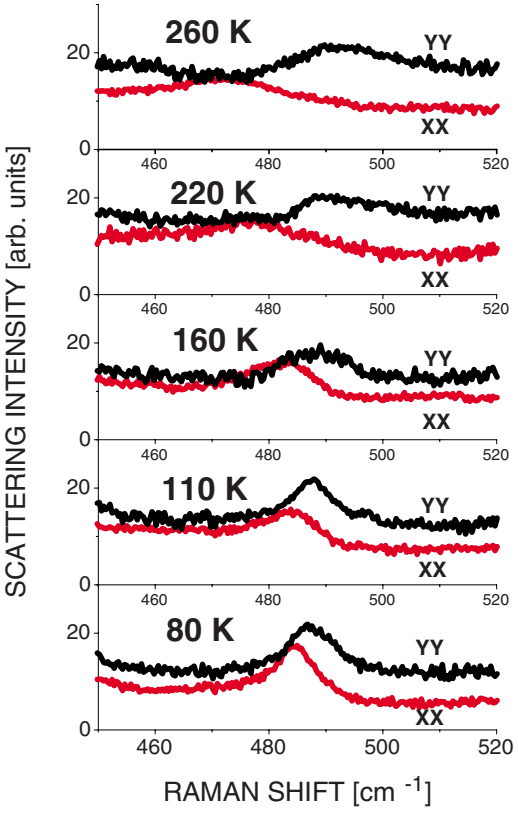

FIG. 6. (Color online) Variation with T of the profile of the Raman line associated with the A_g apex oxygen mode.

ing is formed at $\omega_{\max}=2\Delta$. For underdoped YBCO, a slight decrease in electronic scattering intensity at $\omega<600$ cm^{-1} has been observed below a characteristic temperature T^* well above T_c, and this has been considered a manifestation of a pseudogap opening.[25] There are to our knowledge no reports on the variation in electronic scattering near T^*.

With a few exceptions,[23,27] in experimental studies of the electronic scattering in YBCO, twinned samples have been used and the theoretical models are based on the tetragonal approximation for the crystal structure.

Figures 4 and 5 illustrate that the electronic scattering from the *ab* surface of the ortho-II crystal is strongly anisotropic and temperature dependent below 600 cm^{-1}. Its intensity in the $z(YY)\bar{z}$ spectra is stronger by a factor of 2 than in the $z(XX)\bar{z}$ spectra and much stronger than in the $z(XY)\bar{z}$, $z(X'Y')\bar{z}$, $x(ZZ)\bar{x}$, and $x(YZ)\bar{x}$ spectra. We attribute the stronger electronic Raman intensity for the YY polarization to the additional scattering channels involving two CuO_2 planar bands and a CuO chain band crossing the Fermi surface along the $\Gamma(0,0,0)$-$Y(0,\pi,0)$ direction[28] in the Brillouin zone.

The coupling of the phonons to the electronic excitations contributing to the Raman background is manifested in our spectra by the asymmetric Fano profile of some of the A_g phonon lines, which is most clearly pronounced for those near 118 cm^{-1}(Ba), 168 cm^{-1} (Y), and 486 cm^{-1} (apex oxygen), which interestingly include mainly the motions of atoms that do not belong to the Cu-O planes. For a phonon coupled to an electronic background, the Fano profile

$$I(\omega) = I_0 \frac{(\epsilon + q)^2}{(1+\epsilon^2)} + B(\omega) \tag{1}$$

is generally used to describe the line shape, where $\epsilon=(\omega-\omega_p)/\Gamma$, ω_p is the renormalized phonon frequency that includes all contributions resulting from the interaction of the phonon with elementary excitations, Γ is the linewidth, q is the asymmetry parameter, and $B(\omega)$ is the noninteracting with the phonon part of the electronic excitation continuum. In the case of real phonon and electronic scattering amplitudes t_p and t_e and a flat scattering background around the phonon frequency,

$$\frac{1}{q} = \frac{t_e}{t_p} \pi \rho(T) V, \tag{2}$$

where $\rho(T)$ is the density of electronic excitations coupled to the particular phonon and V is the related electron-phonon coupling constant, and the intensity of the interacting with the phonon part of the electronic continuum in Eq. (1) can be expressed as $I_0=\pi\rho t_e^2$. Under the reasonable assumption that t_e, t_p, and V are only weakly dependent on T, the variations with temperature of the absolute value of $1/q$ and I_0 will be mainly governed by $\rho(T)$. Figure 6 shows in more detail the variations between the 260 and 80 K profiles of the Raman line near 485 cm^{-1}, which corresponds to the apex oxygen A_g mode. In contrast to the known results for twin-free ortho-I crystals, the slopes of Fano shaped profiles in the XX and YY spectra of ortho II are of opposite signs, which is not

surprising if we take into account that $t_p^{xx} \propto \alpha_{xx}$ and $t_p^{yy} \propto \alpha_{yy}$ are of opposite signs for this mode. It is also evident from Fig. 6 that the Raman lines become more symmetric at lower temperatures. The Fano fit of the experimental profiles showed that the $1/q$ factor for *XX* and *YY* decreases, respectively, from −0.6 and +0.8 at 300 K to −0.2 and +0.1 at 80 K. On the other hand, the electronic background $B(\omega,T)$ remains nearly constant between 300 and 200 K but with further cooling significantly decreases between 200 and 100 K (Fig. 5). On the basis of considerations above concerning $1/q(T)$ and $I_0(T)$ being governed by $\rho(T)$, one therefore concludes that with decreasing temperature the density of electronic excitations coupled to this phonon also decreases, concurrently with the decrease in the electronic background $B(\omega,T)$ already noticed. Such a temperature behavior of the electronic Raman scattering is consistent with an opening of a gap in the electronic excitations as the pseudogap in the underdoped high temperature superconductors,[29–31] although no firm conclusion can be done by studying only one sample at one doping. It is worth noting here that the characteristic temperature $T^* \approx 150$ K, below which Opel *et al.*[25] observed a weak spectral weight loss in the $z(XY)\bar{z}$ spectra of twinned films of $YBa_2Cu_3O_{6.5}$ ($T_c \approx 60$ K), is in the same temperature range.

IV. CONCLUSIONS

The experimental results reported here strongly suggest that some of the previous Raman scattering data[12,20,25] obtained from aged twinned surfaces of $YBCO_x$ ($x \approx 6.5$) samples may not be representative of the ordered ortho-II structure. This study provides more reliable data for identification of the ortho-II Raman modes, as well as information on the variation in electronic scattering and electron-phonon interactions within the temperature range where the opening of a pseudogap has been claimed.

ACKNOWLEDGMENTS

This work was supported in part by the State of Texas through the Texas Center for Superconductivity at the University of Houston (TcSUH) and by the U.S. Air Force Office of Scientific Research (SPRING Award ID No. FA9550-06-1-0401). The work at the University of Sherbrooke was supported by the Natural Sciences and Engineering Research Council of Canada and the Fonds Québécois de la Recherche sur la Nature et les Technologies.

[1] R. Liang, D. A. Bonn, and W. N. Hardy, Physica C **336**, 57 (2000).
[2] C. Stock, W. J. L. Buyers, Z. Tun, R. Liang, D. Peets, D. Bonn, W. N. Hardy, and L. Taillefer, Phys. Rev. B **66**, 024505 (2002).
[3] C. Stock, W. J. L. Buyers, R. Liang, D. Peets, Z. Tun, D. Bonn, W. N. Hardy, and R. J. Birgeneau, Phys. Rev. B **69**, 014502 (2004).
[4] M. v. Zimmermann, J. R. Schneider, T. Frello, N. H. Andersen, J. Madsen, M. Kall, H. F. Poulsen, R. Liang, P. Dosanjh, and W. N. Hardy, Phys. Rev. B **68**, 104515 (2003).
[5] N. Gedik, J. Orenstein, R. X. Liang, D. A. Bonn, and W. Hardy, Physica C **408-410**, 690 (2004).
[6] N. Gedik, P. Blake, R. C. Spitzer, J. Orenstein, Ruixing Liang, D. A. Bonn, and W. N. Hardy, Phys. Rev. B **70**, 014504 (2004).
[7] J. Hwang, J. Yang, T. Timusk, S. G. Sharapov, J. P. Carbotte, D. A. Bonn, R. Liang, and W. N. Hardy, Phys. Rev. B **73**, 014508 (2006).
[8] Z. Yamani, B. W. Statt, W. A. MacFarlane, R. X. Liang, D. A. Bonn, and W. N. Hardy, Phys. Rev. B **73**, 212506 (2006).
[9] R. Harris, P. J. Turner, S. Kamal, A. R. Hosseini, P. Dosanjh, G. K. Mullins, J. S. Bobowski, C. P. Bidinosti, D. M. Broun, R. Liang, W. N. Hardy, and D. A. Bonn, Phys. Rev. B **74**, 104508 (2006).
[10] N. Doiron-Leyraud, C. Proust, D. LeBoeuf, J. Levallois, J. B. Bonnemaison, R. X. Liang, D. A. Bonn, W. N. Hardy, and L. Taillefer, Nature (London) **447**, 565 (2007).
[11] M. Iliev, C. Thomsen, V. Hadjiev, and M. Cardona, Phys. Rev. B **47**, 12341 (1993).
[12] O. V. Misochko, S. Tajima, S. Miyamoto, and N. Koshizuka, Solid State Commun. **92**, 877 (1994).
[13] M. N. Iliev, V. G. Hadjiev, and V. G. Ivanov, J. Raman Spectrosc. **27**, 333 (1996).
[14] E. Faulques and V. G. Ivanov, Phys. Rev. B **55**, 3974 (1997).
[15] M. Iliev, H.-U. Habermeier, M. Cardona, V. G. Hadjiev, and R. Gajic, Physica C **279**, 63 (1997).
[16] M. N. Iliev, P. X. Zhang, H.-U. Habermeier, and M. Cardona, J. Alloys Compd. **251**, 99 (1997).
[17] M. Osada, M. Käll, J. Bäckström, M. Kakihana, N. H. Andersen, and L. Börjesson, Phys. Rev. B **71**, 214503 (2005).
[18] S. I. Bredikhin, G. A. Emelchenko, V. S. Shechtman, A. A. Zhokhov, S. Carter, R. J. Chater, J. A. Kilner, and B. C. H. Steele, Physica C **179**, 286 (1991).
[19] K. Conder, Mater. Sci. Eng., R. **32**, 41 (2001).
[20] D. Palles, N. Poulakis, E. Liarokapis, K. Conder, E. Kaldis, and K. A. Müller, Phys. Rev. B **54**, 6721 (1996).
[21] S. Hong, K. Kim, H. Cheong, and G. Park, Physica C **454**, 82 (2007).
[22] Y. B. Li, L. F. Cohen, A. D. Caplin, R. A. Stradling, W. Kula, R. Sobolewski, and J. L. MacManus-Driscoll, J. Appl. Phys. **80**, 2929 (1996).
[23] T. Strohm and M. Cardona, Phys. Rev. B **55**, 12725 (1997).
[24] A. Bock, Ann. Phys. **8**, 441 (1999).
[25] M. Opel, R. Nemetschek, C. Hoffmann, R. Philipp, P. F. Müller, R. Hackl, I. Tüttő, A. Erb, B. Revaz, E. Walker, H. Berger, and L. Forró, Phys. Rev. B **61**, 9752 (2000).
[26] T. Devereaux and R. Hackl, Rev. Mod. Phys. **79**, 175 (2007).
[27] M. Krantz and M. Cardona, J. Low Temp. Phys. **99**, 205 (1995).
[28] E. Bascones, T. M. Rice, A. O. Shorikov, A. V. Lukoyanov, and V. I. Anisimov, Phys. Rev. B **71**, 012505 (2005); I. S. Elfimov, G. A. Sawatzky, and A. Damascelli, *ibid.* **77**, 060504(R) (2008).
[29] T. Timusk and B. W. Statt, Rep. Prog. Phys. **62**, 61 (1999).
[30] M. Le Tacon, A. Sacuto, A. Georges, G. Kotliar, Y. Gallais, D. Colson, and A. Forget, Nat. Phys. **2**, 537 (2006).
[31] V. Hinkov, P. Bourges, S. Pailhes, Y. Sidis, A. Ivanov, C. D. Frost, T. G. Perring, C. T. Lin, D. P. Chen, and B. Keimer, Nat. Phys. **3**, 780 (2007).